Thermodynamics of the Au49Ag5.5Pd2.3Cu26.9Si16.3 glass-forming alloy

(Article begins on next page)

10 April 2024

Thermodynamics of the $Au_{49}Ag_{5.5}Pd_{2.3}Cu_{26.9}Si_{16.3}$ glass-forming alloy

G. Dalla Fontana, G. L. Fiore, L. Battezzati *

Università di Torino, Dipartimento di Chimica, Via Giuria 9, 10125, Torino, Italy

* Corresponding Author: e-mail: livio.battezzati@unito.it, tel +390116707567, fax +390116707855

Abstract

The thermodynamic properties of $Au_{49}Ag_{5.5}Pd_{2.3}Cu_{26.9}Si_{16.3}$, the best Au-based glass-former, were investigated using differential scanning calorimetry. The specific heats of the amorphous, undercooled liquid, and crystal phases and enthalpies of transformation were determined. The differences in enthalpy and entropy of the undercooled melt with respect to equilibrium crystalline phases were calculated. The thermodynamic fragility index (mT), introduced by Angell [1] in relation to the loss of entropy of the liquid phase on undercooling to the glass transition temperature, was derived and compared to fragility indexes of both metallic and conventional glass formers; in particular with another gold alloy, $Au_{77}Ge_{13.6}Si_{9.4}$. Furthermore it was correlated to the kinetic one obtained from dynamic measurements [2].

Keywords: Metallic glasses, Au amorphous alloys, Thermodynamic properties, Melt fragility, Differential scanning calorimetry.

1. Introduction

The metallic glass $Au_{49}Ag_{5.5}Pd_{2.3}Cu_{26.9}Si_{16.3}$ has a glass transition temperature, Tg, well manifest in differential scanning calorimeter (DSC) measurements and a wide supercooled liquid region, ΔT, ($\Delta T = T_x - T_g$, where T_x is the crystallization temperature). Moreover, it melts at low temperature, Tm, because its composition is close to that of a deep eutectic [3]. These features confer to the alloy good glass formability also in bulk form. Both supercooled (metastable) and stable liquid

states are, therefore, accessible to DSC measurement which will give a full range of thermodynamic properties.

Early studies on Au-Si [4] and Au-Ge-Si [5] alloys provided the first data on the properties of glass-forming melts: enthalpy and entropy of fusion, specific heat and viscosity although in limited temperature ranges. Collecting data for the quinary alloy now available, allows for an extended comparison of Au-based metallic glasses with various compositions of bulk glass-formers. In this respect, the concept of melt fragility put forward by Angell, either as a thermodynamic [1] and a kinetic parameter [6], has proved useful in getting insight into the issue of the glassy state both for inorganic and organic materials [7, 8].

In this letter the thermodynamic properties of $Au_{49}Ag_{5.5}Pd_{2.3}Cu_{26.9}Si_{16.3}$ are reported and used to derive the fragility of this alloy in the general framework of glass formers.

2. Experimental

The $Au_{49}Cu_{26.9}Ag_{5.5}Pd_{2.3}Si_{16.3}$ master alloy was prepared from a mixture of the pure elements by arc-melting under Argon atmosphere. Amorphous ribbons and cylinders were obtained by melt spinning and copper mould casting, respectively [9]. X-ray diffraction patterns (Cu-Kα radiation) of samples gave only halo reflections, characteristic of amorphous materials. DSC (Perkin Elmer Pyris Diamond) was used under high purity Argon atmosphere to detect significant temperatures and enthalpies. The specific heat capacity (C_p) of the amorphous, supercooled liquid and crystalline phases were measured by comparison with the specific heat capacity of a sapphire standard using the scanning method: scans with the sample, the sapphire and empty crucibles were performed in defined temperature ranges at 20°C/min between two isothermal arrests of 240 minutes. The calorimeter was also calibrated by measuring the temperature and heat of fusion if pure In and Zn at various scanning rates. The difference in specific heat between liquid and crystal

phases at the temperature of completion of the glass transition were determined by DSC with scanning rates from 0.3 to 100 K/min.

3. Results

Fig.1. shows the DSC trace for a ribbon of the alloy we are analyzing; cylinders display the same features. The glass transition is manifest at 398 K. Exothermal crystallization occurs at about 453. Further minor exothermal effects are detected on heating up to the melting range. The supercooled liquid region, ΔT (T_x-T_g), is of the order of 55 K at the scanning rate of 20 K/min. Eutectic melting occurs at 620 K and the liquidus (T_l) is detected at 694 K (see inset of Fig. 1). The solidification trace has asimilar sequence of signals, but occurring with undercooling of some tens of degrees (Fig. 1). Integrating the area of the peaks as a function of time using a sigmoidal base line, we find the melting enthalpy, crystallization and solidification enthalpy. Tab. 1 lists the thermal data for the $Au_{49}Ag_{5.5}Pd_{2.3}Cu_{26.9}Si_{16.3}$ alloy.

Fig. 2 shows data on specific heat capacities of liquid, supercooled liquid and crystalline states of the alloy. Moreover, the difference in specific heat between liquid and crystal phases was measured at different scanning rates at the respective Tg and was added to the crystal specific heat. Points referring to this are also plotted. The data of the solid specific heat capacity, C_p^s, are fitted using the following relationship:

$$C_p^s = 3R + aT + bT^2 \quad (1)$$

and the undercooled liquid specific heat capacity C_p^l is fitted with [10, 11]

$$C_p^l = 3R + cT + dT^{-2} \quad (2)$$

where R is the universal gas constant, T is the absolute temperature and a, b, c, d are fitting constants. Their values are summarized in Table 2. Empirical equations 1 and 2 are valid well above the Debye temperature as in the case of the present data. The 3R term refers to the Dulong-Petit rule for the specific heat of solids at room

temperature. The temperature dependence of C_p^s is expressed according to classical models [12]. The T^{-2} term in eq. 2 accounts for the rise in specific heat of glass-forming melts on undercooling.

The solid specific heat is 1 to 2 units higher than that obtained by Neumann Kopp's law (the sum of Cp of individual elements times their molar fractions) [12]. C_p^l decreases with increasing temperature as expected for glass-formers.

The consistency of data has been verified according to the following thermodynamic cycle where ΔC_p^{l-s} is the difference in specific heat between liquid and crystal phases:

$$\Delta H_m - \Delta H_x = \int_{T_x}^{T_m} \Delta C_p^{l-s} dT \quad (3)$$

The two terms coincide within the experimental error (Fig. 3a). Analogously, the difference in entropy has been calculated in the reference state of the equilibrium crystalline phases (Fig. 3b)

$$\Delta S = \Delta S_m - \int_{T}^{T_m} \Delta C_p \frac{dT}{T} \quad (4).$$

Liquid entropy is lost on undercooling until the Kauzmann temperature, T_K (Tab. 1), is reached, where the entropy difference between liquid and crystal phases would become nil should not the material escape the paradox by becoming a glass at Tg.

4. Discussion

The loss in ΔH and ΔS on undercooling depends on the behavior of the ΔC_p^{l-s} function, so the specific heat trend reflects the thermodynamic liquid fragility expressed with the parameter, mT, [13] according to

$$m_T = \left[\frac{d \dfrac{\Delta S_g}{\Delta S}}{d \dfrac{T_g}{T}} \right]_{T=T_g} \quad (5).$$

This is expected to correspond to the kinetic fragility, i. e. the slope of the viscosity

function, η, at T_g in the frame of the Adam-Gibbs model of liquid glass-formers [6]

$$m = \left[\frac{d \log(\eta)}{d \frac{T_g}{T}} \right]_{T=Tg} \quad (6).$$

Using equation (2), it is easily proven that m_T is given by $\Delta C_p(T_g)/\Delta S_g$, where ΔS_g is the entropy difference between liquid and stable crystal phases at the experimental T_g. From a statistical analysis based on the Potential Energy Landscape model (PEL) assuming either an hyperbolic or a Gaussian distribution of energy minima of the states explored by liquid configurations, the kinetic fragility index has been derived, respectively, as [14][15]

$$m = 17 \frac{T_g}{T_g - T_K} \quad (7)$$

and

$$m = 17 \frac{T_g^2 + T_k^2}{T_g^2 - T_k^2} \quad (8)$$

The factor 17 refers to the decimal logarithmic range of viscosity from the high temperature limit ($\eta \approx 10^{-5}$ Pa·s) to T_g ($\eta \approx 10^{12}$ Pa·s) derived in [14]. Such factor can be modified in case a different ansatz is made for the quantity η_0. The plot of m as a function of T_g/T_K, lines representing eqs. (7-8), is shown in Fig. 4 where the data are the same as in [8] and the points relative to $Au_{49}Ag_{5.5}Pd_{2.3}Cu_{26.9}Si_{16.3}$ are added. For this alloy the kinetic fragility obtained from viscosity measurements is 52.8 [16], close to that, 46, calculated by means of the span of the glass transition range in DSC runs [2]. The values derived from eq. (5) or, equivalently, eqs. (7-8), span a range from 88 to 107 depending on whether the entire envisaged range of viscosity is considered (i. e. 17 decades) or the experimental range for metallic glasses is taken (i. e. $\eta \approx 10^{-4}$Pa·s at high temperature to $\eta \approx 10^{10}$ Pa·s at the T_g obtained in DSC at the conventional rate of 20

K/min [2, 16]). There is clearly a general discrepancy between the values for metallic with respect to inorganic and organic glasses conforming better to eqs. (7-8). Angell approximated the m_T parameter as

$$m_T = 56 \frac{T_g \Delta C_{p,g}}{\Delta H_m} \quad (9)$$

where $\Delta C_{p,g}$ is the difference of specific heat at glass transition temperature, ΔH_m the melting enthalpy and the 56 is an empirical correlation parameter [18]. Using this relationship the value of thermodynamic fragility of the present Au alloy becomes 71 ± 9. The large deviation of thermodynamic fragility indexes appears related to the quantities employed to compute them and to their relative scatter. The largest uncertainty refers to $\Delta C_p(T_g)$ mostly because of an extra endothermic contribution due to structural relaxation which in turn affects the calculation of ΔS_g and, therefore, the ratio of these quantities. Moreover, the T^{-2} dependence appears to overestimate the liquid specific heat in the experimentally inaccessible region between T_g and T_K causing overestimate of T_K.

Actually, if T_0, the temperature where viscosity should diverge in the Vogel-Fulcher-Tammann equation for η, is employed instead of T_K in a plot of m vs T_g/T_0, a satisfactory agreement between data points and eqs. (7-8) is found [16]. Notwithstanding these uncertainty, the present results reposition Au based metallic glasses within the general behaviour of amorphous alloys explaining the deviation of the m parameter of $Au_{77}Ge_{13.6}Si_{9.4}$ (Fig. 4) [17]. The calculation of T_K in the reference state of crystal phases, i. e. Au and Ge-Si solid solution, via eq. (6), implies the use of the entropy of fusion [18] which includes a contribution due to the transition from a semiconducting to a metallic crystal of the Ge-Si phase. This is inappropriate since the glass is metallic. On the contrary, the equilibrium state of $Au_{49}Cu_{26.9}Ag_{5.5}Pd_{2.3}Si_{16.3}$ is made almost entirely of a mixture of metallic

phases (solid solutions and silicides) [2], therefore its entropy of fusion conforms to the general behavior of metals and, as a consequence, the T_K falls in a different range with respect to the former alloy (Fig. 4).

5. Conclusions

The thermodynamics of the $Au_{49}Ag_{5.5}Pd_{2.3}Cu_{26.9}Si_{16.3}$ bulk glass former has been investigated providing a consistent set of data on transformation enthalpies and specific heats.

The specific heat in the supercooled liquid region was determined in a range of about 40 degrees before alloy crystallization. C_p^l decreases with increasing temperature and a single functional dependence could be employed for the low and high temperature branches of data. Using the full set of data, the enthalpy and entropy trends of the undercooled liquid were computed in the reference state of the equilibrium crystalline phases obtaining an estimate of the Kauzmann temperature. The melt fragility has been obtained employing various parameters based on Angell's approximate formula (6) and on the PEL model of the liquid showing that the present alloy conforms to the general behaviour of metallic glass formers, contrary to Au-GeSi melts. The large scatter in fragility indexes seems to indicate that the T^{-2} dependence of the liquid specific heat should be reconsidered in order to get a better agreement between T_K and T_0 temperatures.

Acknowledgements

References

[1] L.M. Martinez, C.A. Angell, Nature 410 (2001) 663-667.

[2] G. Fiore, I. Ichim, L. Battezzati, J. Non-Cryst. Solids. 356 (2010) 2218-2222.

[3] J. Schroers, Appl. Phys. Lett. 87 (2005) 061912.

[4] W. Klement, R.H. Willens, P. Duwez, Nature 187 (1960) 869-870.

[5] HS. Chen, D. Turnbull, J. Chem. Phys. 48 (1968) 2560-2571.

[6] C.A. Angell, Science 267 (1995) 1924–1935.

[7] L. Battezzati, G. Dalla Fontana, J. Alloys Comp. (2012),

http://dx.doi.org/10.1016/j.jallcom.2012.10.027

[8] G. Dalla Fontana, L. Battezzati, Acta Mater. 61 (2013) 2260–2267

[9] G. Fiore, I. Ichim, L. Battezzati, J. Phys.: Conference Series 144 (2009) 012039.

[10] S.C. Glade, R. Busch, D.S. Lee, W.L. Johnson, R.K. Wunderlich, H.J. Fecht, J. Appl. Phys. 87 (2000) 7242-7248.

[11] R. Busch, Y.J. Kim, W.L. Johnson, J. Appl. Phys. 77 (1995) 4039-4043.

[12] A.T. Dinsdale, Calphad 15 (1991) 311-425.

[13] L.M. Wang, C.S. Angell, R. Ranko, J. Chem. Phys. 125 (2006) 074505.

[14] G. Ruocco, F. Sciortino, F. Zamponi, C. De Michele, T. Scopigno, J. Chem. Phys. 120 (2004) 10666-10680.

[15] L. Battezzati, J. Alloy Comp. 495 (2010) 294-298.

[16] J. Schroers, Acta Mater. 56 (2008) 471-478.

[17] D. N. Perera, J Phys: Condens. Matter 11 (1999) 3807.

[18] L.M. Wang, C.S. Angell, R.Richet, J. Chem. Phys 125 (2006) 074505

Figure captions

Fig. 1. DSC trace given by an amorphous ribbon of $Au_{49}Ag_{5.5}Pd_{2.3}Cu_{26.9}Si_{16.3}$ at the heating rate of 20 K/min. Insets show details of melting (top, curve obtained on heating) and solidification (bottom, curve obtained on cooling).

Fig. 2. Specific heat capacity of $Au_{49}Ag_{5.5}Pd_{2.3}Cu_{26.9}Si_{16.3}$. The light blue and red squares are experimental points obtained with the master alloy, amorphous cylinders and ribbons. The red line is the fit to points with eq. (1) and the blue on with eq. (2). Triangles give the sum of the difference in specific heat obtained by

measuring the step of DSC signal at T_g at different scanning rates and of the crystal specific heat. The error bar refers to the maximum scatter of points.

Fig. 3. Variation of enthalpy (a) and entropy (b) of undercooled liquid calculated in the reference state of the equilibrium crystalline phases. The red squares are the experimental points on crystallization enthalpy. At T_m the error bar for enthalpy derives from a set of experiments; at T_g the bar refers to error propagation of both enthalpy and specific heat.

Fig. 4. The fragility parameter m for metallic (full circles) [16] and non-metallic (open circles) [16] as a function of the ratio T_g/T_K. Dashed and full lines computed with eqs. (7-8). For $Au_{49}Ag_{5.5}Pd_{2.3}Cu_{26.9}Si_{16.3}$ (here called A5 for brevity) m values are reported as obtained from viscosity [16] (blue full circle) and from the span of the glass transition temperature at 20 K/min (red full circle) [2]. Error bars are computed from typical available uncertainty of experimental quantities.

Table captions:

Tab. 1. Thermal properties of $Au_{49}Ag_{5.5}Pd_{2.3}Cu_{26.9}Si_{16.3}$: Kauzmann, T_K, glass transition, T_g, crystallization, T_x, eutectic, T_m, liquidus, T_l, solidification start, T_s, temperatures and the enthalpies of melting, ΔH_m, and solidification, ΔH_s.

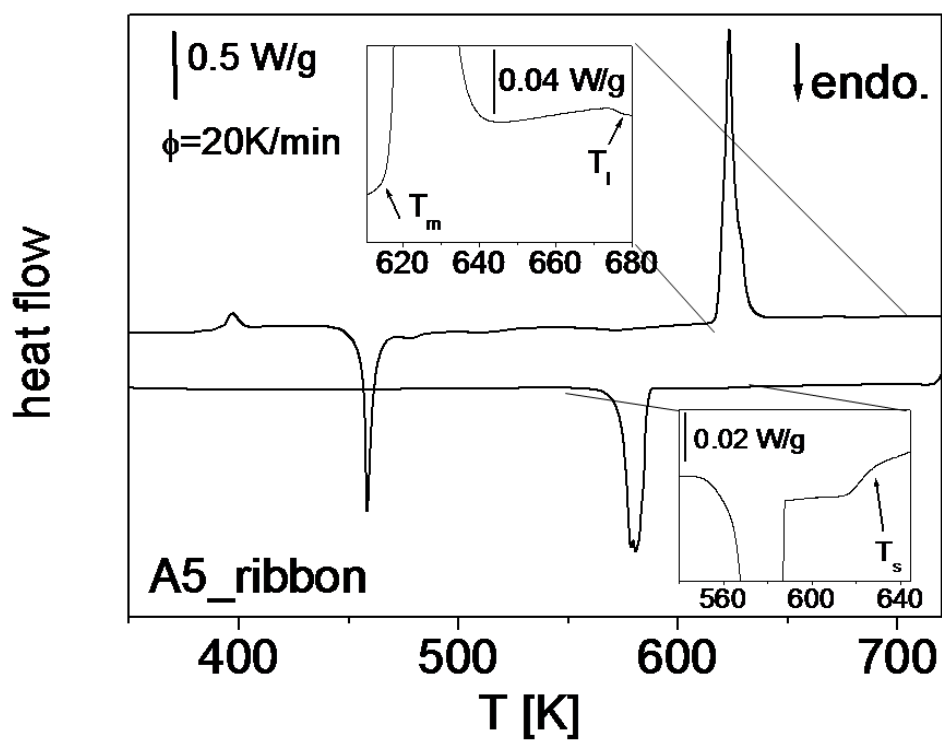Tab. 2. The specific heat capacity parameters for the liquid and the crystalline state.
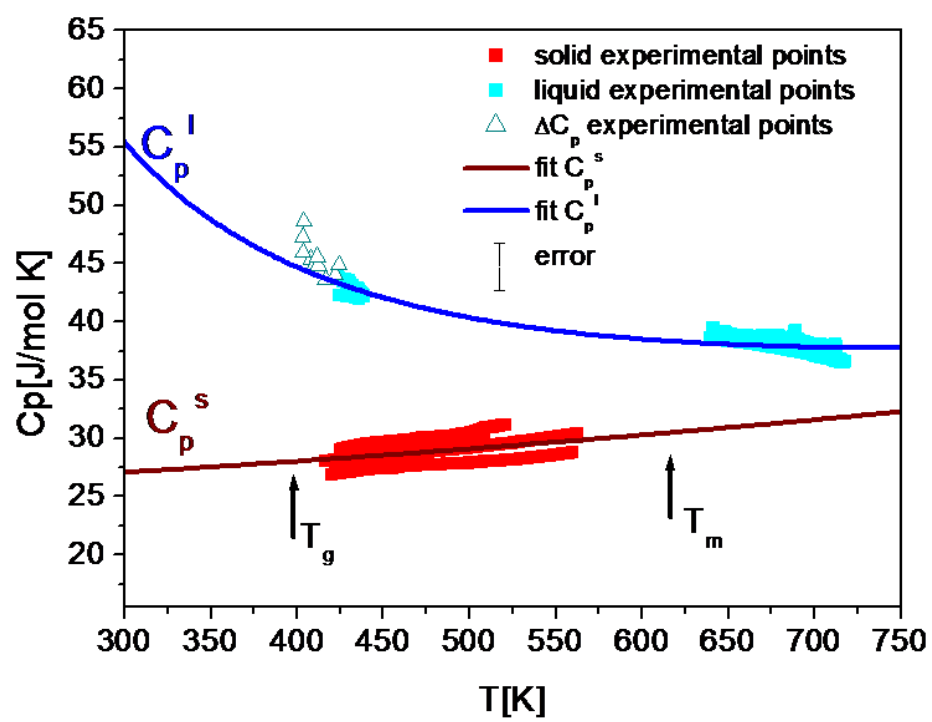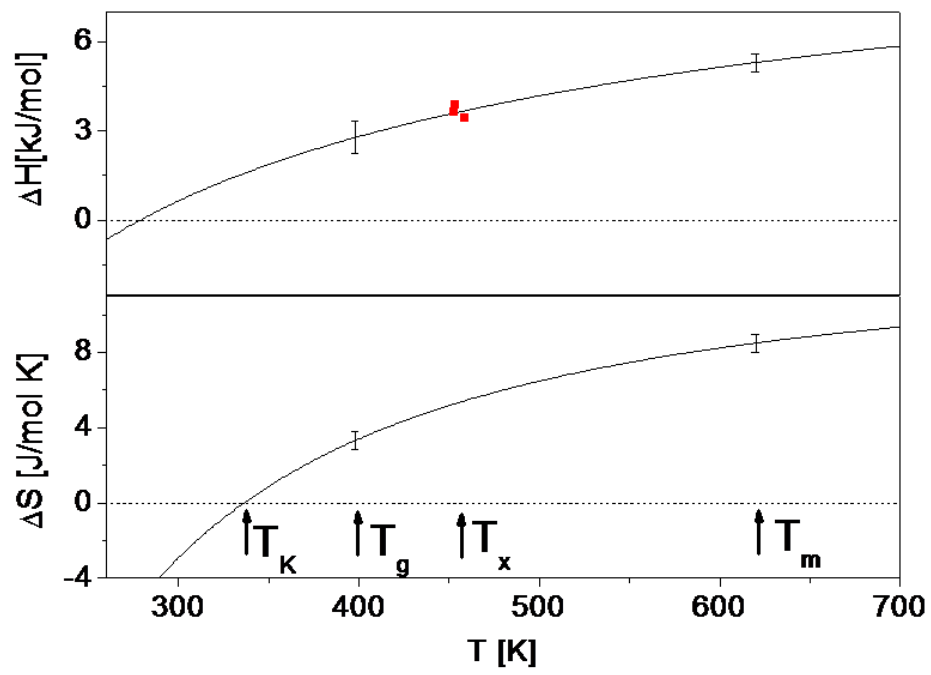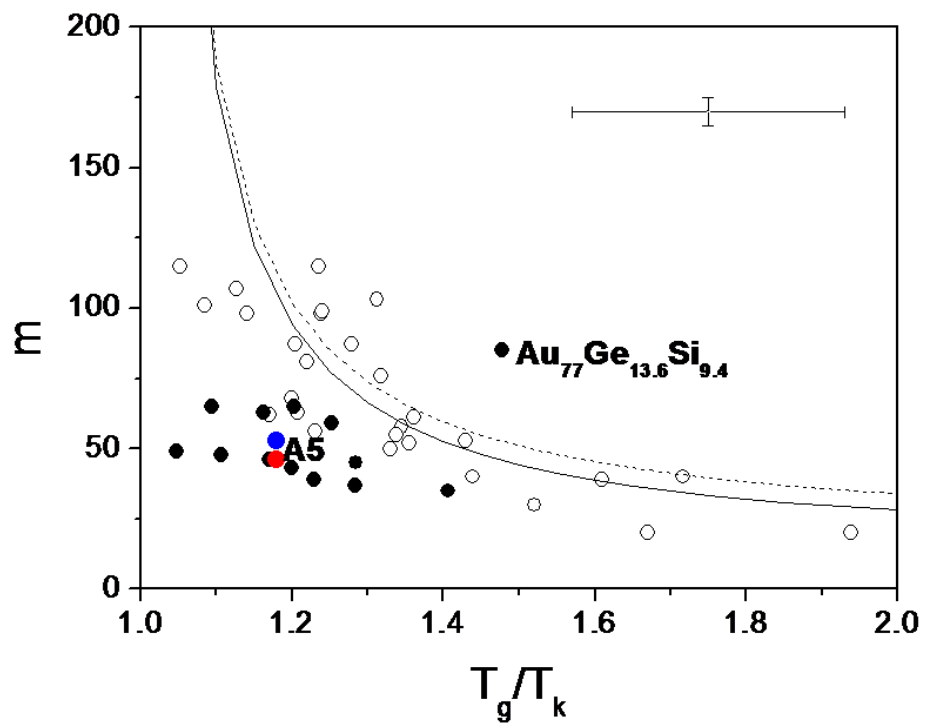
Fig. 1.

Fig. 2.

Fig.3.

Fig. 4.

Fig.5.
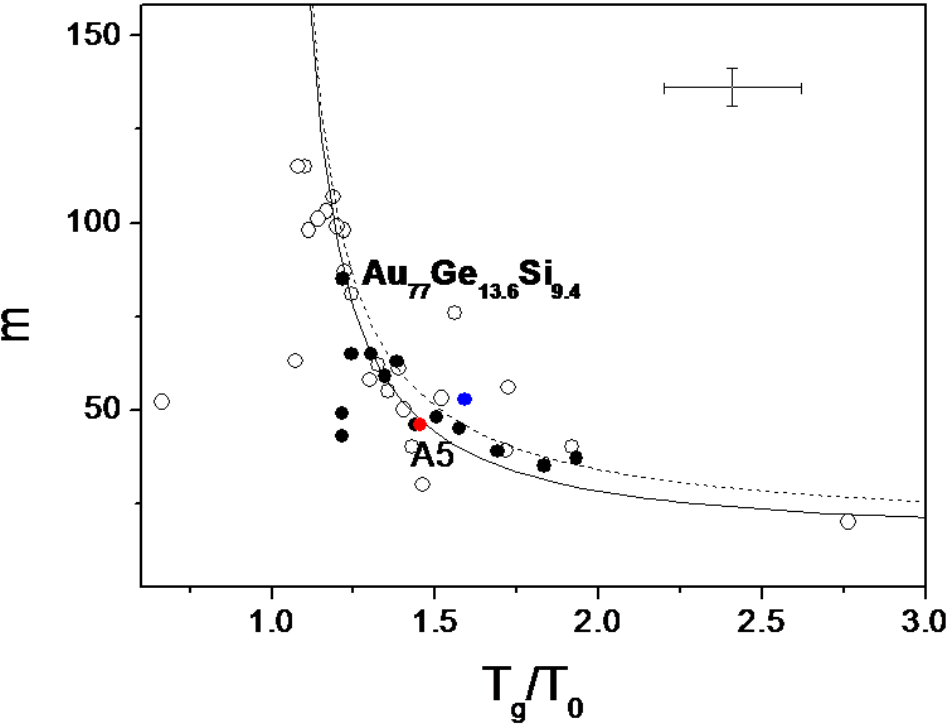
Tab.1.

T_k [K]	T_g [K]	T_x [K]	T_m [K]	T_l [K]	T_s K]	ΔH_m [kJ/mol]	ΔH_s [kJ/mol]	ΔH_x [kJ/mol]
335	398±3	453±3	620±2	694±9	630±4	5.3±0.3	8.5±0.2	3.6 ±0.3

Tab.2.

	a [J mol^{-1}K^{-2}]	b [J mol^{-1}K^{-3}]	c [J mol^{-1}K^{-2}]	d [J mol^{-1}K]
A5	5.23447X10^{-3}	6.02849X10^{-6}	1.126583X10^{-2}	2.439524X10^{6}